Pressure induced charge disproportionation in $LaMnO_3$

2004 J. Phys.: Condens. Matter 16 S5633

(http://iopscience.iop.org/0953-8984/16/48/020)

INSTITUTE OF PHYSICS PUBLISHING JOURNAL OF PHYSICS: CONDENSED MATTER

J. Phys.: Condens. Matter **16** (2004) S5633–S5637 PII: S0953-8984(04)83055-8

Pressure induced charge disproportionation in $LaMnO_3$

G Banach and W M Temmerman

Daresbury Laboratory, Daresbury, Warrington WA4 4AD, UK

Received 2 July 2004
Published 19 November 2004
Online at stacks.iop.org/JPhysCM/16/S5633
doi:10.1088/0953-8984/16/48/020

Abstract

We present a study of total energy as a function of volume in the cubic phase of $LaMnO_3$. A state of charge disproportionation into planes of $Mn^{3+}O_2/Mn^{4+}O_2$ was found. It is argued that the pressure driven localization/delocalization transition might go smoothly through a region of Mn^{3+} and Mn^{4+} coexistence.

1. Introduction

The pressure induced quenching of the Jahn–Teller distortion and metal–insulator transition in $LaMnO_3$ were recently studied [1] by means of synchrotron x-ray diffraction, optical spectroscopies and transport measurements under pressures up to 40 GPa. This work stresses that the delocalization of electron states is a key feature of $LaMnO_3$ in the pressure range of 20–30 GPa. In this paper we present calculations which show that the delocalization of electron states goes through a phase of charge disproportionation where Mn^{3+} and Mn^{4+} coexist.

Interest in perovskite manganites [2–4] was recently rekindled due to the observation of 'colossal' negative magnetoresistance in $La_{1-x}CaMnO_3$ [5]. The half-metallic character of $La_{2/3}Sr_{1/3}MnO_3$ [6] is an important factor which results in a magnetoresistance ratio of more than 1800% at 4 K. The phase diagram of $La_{1-x}SrMnO_3$ is complex [7], revealing the competition between the double-exchange and superexchange interactions, charge and orbital ordering instabilities and strong coupling to the lattice deformations. Furthermore, it has been argued that local Jahn–Teller effects, such as random Jahn–Teller distortions of the MnO_6 octahedra [8] and dynamical effects [9], are of importance for explaining the magnetic properties of these materials.

Recently Banach and Temmerman [10] showed that under Sr doping the delocalization transition from the valence Mn^{3+}, as seen in $LaMnO_3$ [11], to the valence Mn^{4+} is characterized by a transition region extending up to 20% Sr where Mn^{3+} and Mn^{4+} coexist in a charge disproportionated state. These LSMO systems were cubic and therefore the Jahn–Teller distortion did not play a role in this. Similar results are also obtained by calculations of Korotin *et al* [12], who show for $La_{7/8}Sr_{1/8}MnO_3$ the occurrence of orbital order and insulating behaviour in the ferromagnetic state without any Jahn–Teller distortion.

In this paper we study whether a delocalization of Mn^{3+} to Mn^{4+} also occurs, under pressure, in the cubic phase of the parent compound $LaMnO_3$ and whether such a pressure induced transition is also characterized by a region of Mn^{3+} and Mn^{4+} coexistence. The Jahn–Teller distortion is ignored in the present study, while it was included in the study of the electronic properties of $LaMnO_3$ by Tyer *et al* [11]; it was found in that work that the Jahn–Teller interaction is the dominant effect in realizing orbital order, which is not considered in this work.

SIC–LSD calculations are performed for $LaMnO_3$ in the ferromagnetic (FM) and antiferromagnetic A (AF-A)—which is the antiferromagnetic ordering in the (001) direction—structures at different volumes to study the localization of the Mn d states. These calculations are performed for different configurations of localized states as a function of volume. In particular, configurations where the 3d Mn t_{2g} states are localized will be considered as well as 3d Mn t_{2g} and 3d Mn e_g of $3z^2 - r^2$ symmetry. By doubling the unit cell in the z-direction we can also investigate in the AF-A structure and a Mn^{3+}/Mn^{4+} charge ordered state with the same structure.

The organization of this paper is as follows. In the next section we explain the SIC–LSD formalism and give some calculational details. The third section contains our results and discussions and the fourth section summarizes the paper.

2. Formalism and calculational details

The basis of the SIC–LSD formalism is a self-interaction free total energy functional, E^{SIC}, obtained by subtracting from the LSD total energy functional, E^{LSD}, a spurious self-interaction of each occupied electron state ψ_α [13], namely

$$E^{\mathrm{SIC}} = E^{\mathrm{LSD}} - \sum_{\alpha}^{\mathrm{occ}} \delta_\alpha^{\mathrm{SIC}}. \tag{1}$$

Here α numbers the occupied states and the self-interaction correction for the state α is

$$\delta_\alpha^{\mathrm{SIC}} = U[n_\alpha] + E_{xc}^{\mathrm{LSD}}[\bar{n}_\alpha], \tag{2}$$

with $U[n_\alpha]$ being the Hartree energy and $E_{xc}^{\mathrm{LSD}}[\bar{n}_\alpha]$ the LSD exchange–correlation energy for the corresponding charge density n_α and spin density $\bar{n}_\alpha$. The SIC–LSD approach can be viewed as an extension of the LSD in the sense that the self-interaction correction is only finite for spatially localized states, while for Bloch-like single-particle states E^{SIC} is equal to E^{LSD}. Thus, the LSD minimum is also a local minimum of E^{SIC}. A question now arises of whether there exist other competitive minima, corresponding to localized states, which could benefit from the self-interaction term without losing too much of the energy associated with band formation. This is often the case for rather well localized electrons such as the 3d electrons in transition metal oxides. It follows from minimization of equation (1) that within the SIC–LSD approach such localized electrons move in a different potential to the delocalized valence electrons, which respond to the effective LSD potential. For example, in the case of manganese, three (Mn^{4+}) or four (Mn^{3+}) Mn d electrons move in the SIC potential, while all other electrons feel only the effective LSD potential. Thus, by including an explicit energy contribution for electron localization, the *ab initio* SIC–LSD describes localized and delocalized electrons on an equal footing, leading to a greatly improved description of static Coulomb correlation effects over the LSD approximation.

In order to make the connection between valence and localization more explicit it is useful to define the nominal valence as

$$N_{\mathrm{val}} = Z - N_{\mathrm{core}} - N_{\mathrm{SIC}},$$

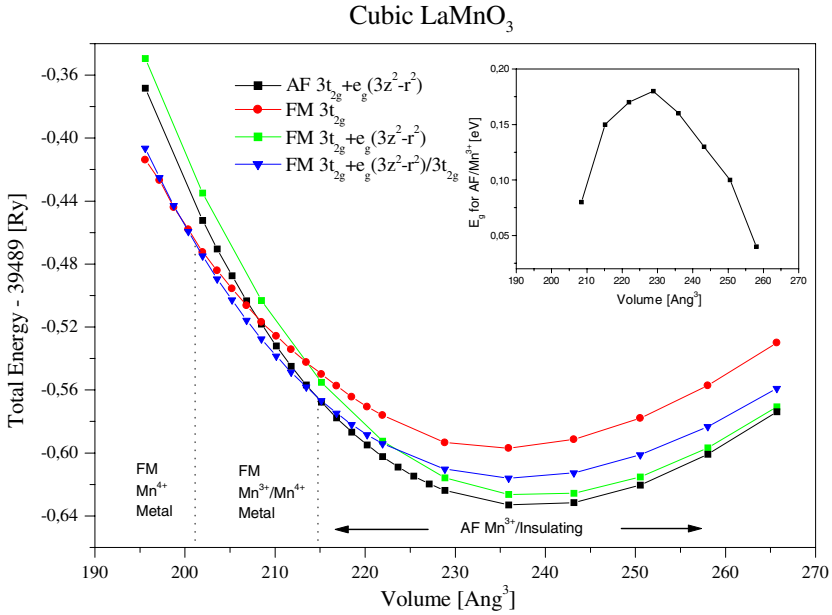

Figure 1. The total energy versus volume for cubic $LaMnO_3$ for four different scenarios of magnetic structure and charge order. These are: antiferromagnetic A and trivalent Mn (with the three t_{2g} electrons and one e_g electron of $d_{3r^2-z^2}$ symmetry localized) (black); ferromagnetic and tetravalent Mn (with the three t_{2g} electrons localized) (red); ferromagnetic and trivalent Mn (with the three t_{2g} electrons and the e_g electron of $d_{3r^2-z^2}$ symmetry localized) (green); the ferromagnetic Mn^{3+}/Mn^{4+} charge disproportionated configuration (blue). The inset shows the band gap versus volume for trivalent Mn in the AF-A structure.

(This figure is in colour only in the electronic version)

where Z is the atomic number (25 for Mn), $N_{\rm core}$ is the number of core (and semi-core) electrons (18 for Mn) and $N_{\rm SIC}$ is the number of localized, i.e., self-interaction corrected, states (either three or four for Mn^{4+} or Mn^{3+}, respectively). Thus, in this formulation the valence is equal to the integer number of electrons available for band formation. To find the valence we assume various atomic configurations, consisting of different numbers of localized states, and minimize the SIC–LSD energy functional of equation (1) with respect to the number of localized electrons. The SIC–LSD formalism is governed by the energetics due to the fact that for each orbital the SIC differentiates between the energy gain due to hybridization of an orbital with the valence bands and the energy gain upon its localization. Which one 'wins' determines whether the orbital is part of the valence band or not and in this manner also leads to the evaluation of the valence of elements involved.

In the present work the SIC–LSD approach has been implemented [14] within the linear muffin-tin-orbital (LMTO) atomic sphere approximation (ASA) band structure method [15], in the tight-binding representation [16].

3. Results and discussion

In figure 1 we show the total energy versus volume for two different magnetic structures and three different states of charge order. These are the ferromagnetic and antiferromagnetic (along the z-direction) magnetic orders. The charge order refers to trivalent Mn^{3+}, tetravalent Mn^{4+}

and a disproportionated state of Mn^{3+}/Mn^{4+}. This disproportionated state Mn^{3+}/Mn^{4+} consists of alternate MnO_2 planes in the (001) direction. The ground state is antiferromagnetic with Mn^{3+} valence in the cubic structure. This result shows that the Jahn–Teller distortion is not a necessary prerequisite for an insulating ground state. Rather, the valence of the Mn ion and the magnetic structure determine the insulating properties. Furthermore, the experimentally observed AF-A magnetic order is obtained in the cubic structure, indicating that the Jahn–Teller distortion does not influence the magnetic structure. Further inspection of figure 1 also reveals that the energy scale associated with the magnetic structure is smaller than the one associated with the charge. In the vicinity of the energy minimum we find that the least unfavourable configuration is trivalent (Mn^{3+}) in the ferromagnetic state, whilst the most unfavourable is tetravalent (Mn^{4+}) in the ferromagnetic structure. The theoretical volume is in very good agreement with experiment: 238 $Å^3$ versus an experimental value of 244 $Å^3$.

Reducing the volume, we obtain between 200 and 215 $Å^3$ a charge disproportionated Mn^{3+}/Mn^{4+} state, in the ferromagnetic structure, as the state with the lowest energy. This state consists of an antiferromagnetic ordering of the MnO_2 planes along the z-direction according to $Mn^{3+}O_2/Mn^{4+}O_2$. Such a state is also observed in Sr doped $LaMnO_3$. In the calculations of Banach and Temmerman [10] this state was obtained by Sr doping whilst keeping the volume constant. The present results demonstrate that the volume reduction is another factor inducing the charge disproportionated state whilst Jahn–Teller distortions, globally or locally, are not necessary. However, this charge order can drive a structural distortion which is still present in $LaMnO_3$ under pressure [1, 17]. Note that we have only studied the simplest of the charge ordered states and that a more complex ordering might give rise to a further lowering of the energy. Obviously this could be modelled by larger supercells; this was not examined in this work.

Consideration of the Jahn–Teller distortion in this volume range would probably introduce the possibility of orbital order, which would be interesting to study as a function of pressure. The occurrence of a charge disproportionated Mn^{3+}/Mn^{4+} region as a function of pressure could lead to local Jahn–Teller distortions and the disappearance of the Jahn–Teller distortion as a function of pressure might therefore not happen uniformly.

When the ferromagnetic charge disproportionated state is entered the system becomes metallic. The polarization is around 70% in this charge disproportionated state. This state persists through the next phase transition into tetravalent Mn^{4+} at a volume of 200 $Å^3$.

The charge disproportionation at the surface might be different from that in the bulk. Calculations were performed to model a $LaMnO_3$ surface by considering a supercell consisting of four $LaMnO_3$ formula units and two 'empty $LaMnO_3$' formula units. The $LaMnO_3$ surface can be terminated with either LaO or MnO_2 planes. Calculations were made for both cases and for a MnO_2 surface the delocalization of the e_g electron took place. This is surprising since one would expect on intuitive grounds, due to band narrowing, a localization at the surface to be preferable. This is the case for example in α-Ce where the surface consists of γ-Ce [18]. That a delocalization at the surface took place is also reflected in a reduction of the Mn surface magnetic moment by 6%. The reason might be that the e_g electron localized in the bulk is of $3r^2 - z^2$ symmetry character and this orbital points perpendicular to the surface into the vacuum. Therefore it has fewer electrons to capture for localization. Changing the surface termination to LaO does not alter the valence on the Mn in the MnO_2 sub-surface; however, it does change the symmetry of the localized state from $d_{3r^2-z^2}$ to $d_{x^2-y^2}$.

4. Summary and outlook

We have calculated the electronic total energy of $LaMnO_3$, in the cubic structure, as a function of volume and for different magnetic and charge ordered states. We find that the Jahn–Teller

distortion is not crucial for explaining the insulating antiferromagnetic ground state of $LaMnO_3$. A smooth localization–delocalization transition is observed, since the transition from Mn^{3+} to Mn^{4+} goes through the intermediary of a mixture of Mn^{3+}/Mn^{4+}. An accurate p–V curve could be modelled via CPA (coherent potential approximation) calculations where at each volume the total energy is minimized with respect to the concentration of Mn^{3+} and Mn^{4+} [19].

Acknowledgments

G Banach was supported by the EU-funded Research Training Network: 'Computational Magnetoelectronics' (HPRN-CT-2000-00143). He also gratefully acknowledges discussions with Drs A Haznar and R Tyer.

References

[1] Loa I, Adler P, Grzechnik A, Syassen K, Schwarz U, Hanfland M, Rozenberg G Kh, Gorodetsky P and Pasternak M P 2001 *Phys. Rev. Lett.* **87** 125501
[2] Ramirez A P 1997 *J. Phys.: Condens. Matter* **9** 8171
[3] Imada M, Fujimori A and Tokura Y 1998 *Rev. Mod. Phys.* **70** 1039
[4] Coey J M D, Viret M and von Molnár S 1999 *Adv. Phys.* **48** 167
[5] Jin S, Tiefel T H, McCormack M, Fastnacht R A, Ramesh R and Chen L H 1994 *Science* **264** 413
[6] Bowen M, Bibes M, Barthelemy A, Contour J-P, Anane A, Lemaitre Y and Fert A 2003 *Appl. Phys. Lett.* **82** 233
[7] Hemberger J, Krimmel A, Kurz T, Krug von Nidda H-A, Ivanov V Yu, Mukhin A A, Balbashov A M and Loidl A 2002 *Phys. Rev.* B. **66** 094410
[8] Dzero M, Gor'kov L P and Kresin V Z 2003 *Int. J. Mod. Phys.* B **17** 2095
[9] Michaelis B and Millis A J 2003 *Phys. Rev.* B. **68** 115111
[10] Banach G and Temmerman W M 2004 *Phys. Rev.* B **69** 054427
[11] Tyer R, Temmerman W M, Szotek Z, Banach G, Svane A, Petit L and Gehring G A 2004 *Europhys. Lett.* **65** 519
[12] Korotin M, Fujiwara T and Anisimov V 2000 *Phys. Rev.* B **62** 5696
[13] Perdew J P and Zunger A 1981 *Phys. Rev.* B **23** 5048
[14] Temmerman W M, Svane A, Szotek Z and Winter H 1998 *Electronic Density Functional Theory: Recent Progress and New Directions* ed J F Dobson, G Vignale and M P Das (New York: Plenum)
[15] Andersen O K 1975 *Phys. Rev.* B **12** 3060
[16] Andersen O K and Jepsen O 1984 *Phys. Rev. Lett.* **53** 2571
[17] Pinsard-Gaudart L, Rodriguez-Carvajal J, Daoud-Aladine A, Goncharenko I, Medarde M, Smith R I and Revcolevschi A 2001 *Phys. Rev.* B **64** 064426
[18] Eriksson O, Albers R C, Boring A M, Fernando G W, Hao Y G and Cooper B R 1991 *Phys. Rev.* B **43** 3137
[19] Lüders M, Ernst A, Däne M, Szotek Z, Svane A, Ködderitzsch D, Hergert W, Györffy B L and Temmerman W M 2004 *Preprint* cond-mat/0406515